NOTES AND CORRESPONDENCE

On the Relative Vorticity of the Atlantic Jet in the Alboran Sea

ÁLVARO VIÚDEZ AND ROBERT L. HANEY

Department of Meteorology, Naval Postgraduate School, Monterey, California

9 June 1995 and 8 March 1996

ABSTRACT

It is shown, from hydrographic data, that the eastward flowing Atlantic jet (AJ) in the Alboran Sea has zero or positive relative vorticity. This holds even when the AJ curves anticyclonically around the western and eastern Alboran gyres. This feature is due to the presence of large positive shear vorticity mainly caused by the interaction between the AJ and the slow westward flow of Mediterranean Water on the northern side of the AJ. It is also shown that the AJ acquires negative curvature vorticity at the same time that it acquires positive shear vorticity at the exit of the Strait of Gibraltar. This feature is described in terms of a shear and curvature conversion. It is found that the cross-stream variation of alongstream geopotential differences is the main term in this vorticity interchange description of the AJ in the western Alboran Sea.

1. Introduction

The large-scale circulation of the Mediterranean is mainly controlled by the excess of evaporation over the freshwater input from precipitation and rivers. As a consequence, a two-layer flow through the Strait of Gibraltar compensates for the water and salt deficit with Atlantic water (AW, $S < 36.5$ psu) flowing into the Alboran Sea in the upper layer (Atlantic jet, hereinafter AJ), and Mediterranean Water (MW, $S > 38.4$ psu) flowing westward below. Being the westernmost Mediterranean subbasin, the Alboran Sea is the first to receive the incoming AW, and it is where the AW is first modified to acquire characteristics intermediate between the underlying MW and the AW above. This water in the Alboran Sea is termed modified Atlantic water (MAW) or Atlantic–Mediterranean interface water (Gascard and Richez 1985).

The circulation of the upper layers in the western Alboran basin (WAB) has been studied intensively in the last two decades. From the first observations of the AJ and the western Alboran gyre (WAG) (Seco 1959; Donguy 1962) until the most recent experimental and numerical results (Perkins et al. 1990; Tintoré et al. 1991; Viúdez et al. 1996a), there has been a considerable amount of observational, numerical, and laboratory research to determine the physical characteristics of the AJ–WAG system and to explain the physical processes involved. After several field experiments in the WAB, the large-scale AJ–WAG system is considered to be a quasi-permanent feature (e.g., Parrilla and Kinder 1987). At smaller scales, jet fluctuations (Perkins et al. 1990), atmospheric forcing (Bucca and Kinder 1984), and mesoscale eddies (Tintoré et al. 1991; Viúdez et al. 1996a) distort this large-scale system.

The above studies notwithstanding, the physical mechanisms responsible for the wavelike nature of the AJ together with the maintenance and variability of the WAG are not clear. Ovchinnikov et al. (1976) attribute the formation of the WAG to the negative vorticity of atmospheric wind stress forcing. Bryden and Stommel (1982) suggest that the upward and westward flow of Mediterranean deep water provides the source of anticyclonic vorticity necessary to maintain the WAG against frictional dissipation. The numerical results of Preller and Hulburt (1982) and Preller (1986), using a reduced-gravity model, suggest that the AJ is a standing Rossby wave. They found that the horizontal dimensions of the WAG were strongly dependent upon the relative vorticity of the incoming AJ, obtaining an enhancement of the gyre by imposing negative relative vorticity on the incoming current. Loth and Crépon (1984), on the other hand, using a quasigeostrophic shallow-water model, found that imposing positive relative vorticity on inflow was necessary for the formation of the model gyre. Wang (1987), using a primitive equations (PE) model, states that the ''strong negative relative vorticity acquired by the inflow as it leaves the Strait of Gibraltar is generated by an upward vertical velocity that compresses the vortex column.'' Werner et al. (1988), in an application to the Alboran Sea,

Corresponding author address: Álvaro Viúdez, Department of Meteorology, Naval Postgraduate School, 589 Dyer Road, Monterey, CA 93943-5114.
E-mail: viudez@met.nps.navy.mil

showed that the reduced-gravity response of a hydraulically formed flow in a rectangular basin depends critically on the form of the boundary conditions on the domain's sidewalls. Speich (1992) concluded that a gain of negative relative vorticity occurs due to the divergence of the flow produced by a sharp variation in the meridional pressure gradient when the AJ passes the strait. The laboratory experiments by Whitehead and Miller (1979) indicate that the growth of the WAG seems to result from an accumulation of fluid from the AJ as it reaches the Moroccan coast (stagnation point) and that the specific features of the African coastline may stop this accumulation and determine the final size of the gyre. Laboratory experiments by Bormans and Garrett (1989) suggest that the key parameter determining whether the exit flow from the Strait of Gibraltar forms a gyre or a coastal jet is the sharpness of the exit corner in relation to the inertial radius u/f, where u is the characteristic flow speed and f is the Coriolis parameter. Laboratory experiments by Klinger (1994) show that the angle of the exit corner must be above a critical value of between 40° and 45° for the gyre to form, concluding that the basic mechanism of gyre formation may be viscous boundary effects.

The above results and suggestions seem to indicate that there exist different driving mechanisms and physical processes related to the different characteristics of the AJ. In particular, arguments based on relative vorticity have been frequently used to explain, or to interpret, numerical and laboratory results that could account for the observed behavior of the AJ and WAG. The aim of this note is, first, to document an important physical characteristic of the AJ in the WAB, namely, that the relative vorticity of the anticyclonically curved AJ actually remains positive all along the jet and, second, to describe in terms of vorticity the gain of anticyclonic curvature by the AJ.

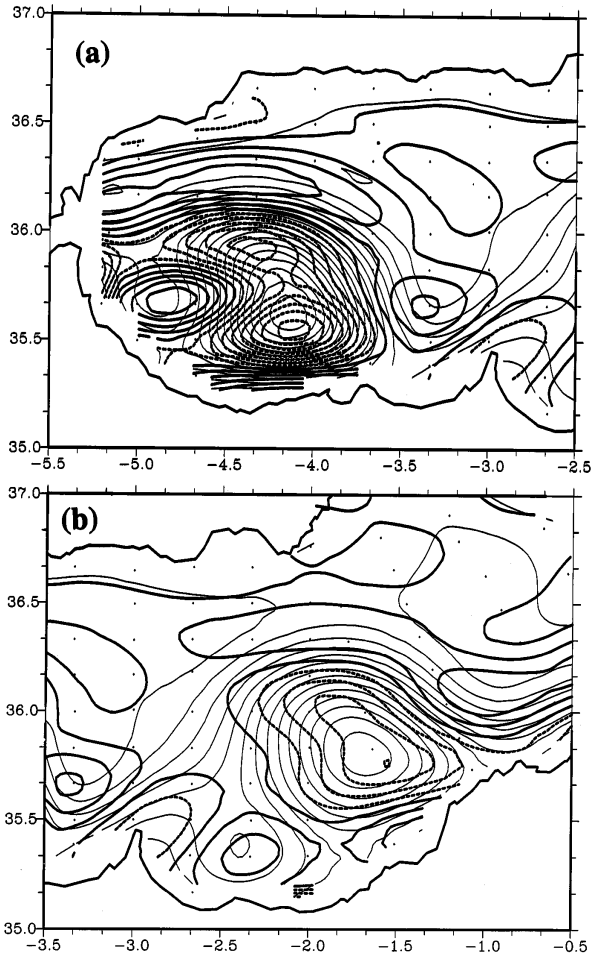

FIG. 1. Geostrophic relative vorticity (thick isolines) and geostrophic streamfunction (thin lines) at 100 m in (a) the western and (b) the eastern Alboran basin. Solid contour lines indicate positive (or zero) relative vorticity ($\Delta = 0.5 \times 10^{-5}$ s^{-1}). The dots indicate the CTD stations.

2. Vorticity in the wavelike jet

The main dataset consists of 134 CTD stations ($\Delta x \approx 30$ km, $\Delta y \approx 18$ km) carried out in the Alboran Sea in September 1992 (Viúdez et al. 1996a). The AJ and both the WAG and eastern Alboran gyre (EAG) in the eastern Alboran basin (EAB) were sampled with the resolution required to compute the geostrophic relative vorticity fields corresponding to the AJ–gyres system. For further reference, a clear definition of the jet and gyre is required. Strictly, the jet and gyre are not two independent physical systems since there is water interchange between them (Lanoix 1974; Viúdez et al. 1996a, 1996b). However, to a first approximation the jet and gyre are in geostrophic balance, and, therefore, closed isolines of the geostrophic streamfunction are used to define unambiguously the WAG and to distinguish it from the AJ (open wavelike isolines). Since an analysis of the separate tendencies for shear and curvature vorticity requires a computation of the ageostrophic velocity, the density data were dynamically assimilated into a primitive equation model (to be explained in the next section). The geostrophic vorticity field presented here was therefore computed from the resulting assimilated density field. To avoid word repetition, and only in this section, velocity, vorticity, etc. mean their respective geostrophic components.

The relative vorticity fields at 100 m in the WAB and EAB [computed using a reference level of 200 m (Lanoix 1974; Perkins et al. 1990)] are shown in Fig. 1. While it is clearly observed that the WAG has zero or negative relative vorticity, the AJ along its anticyclonic curvature has zero or positive relative vorticity. This fact is due to the presence of a strong positive shear vorticity. Curvature and shear vorticity are easily defined using the natural reference frame (**s**, **n**). The frame (**s**, **n**) is the reference frame [in general anholonomic; see, e.g., Marris and Passmann (1968)] of horizontal orthogonal basis vectors defined from the horizontal ve-

locity field (**v**, with $v \neq 0$), such that $\mathbf{s} \equiv \mathbf{v}/v$ is the unit tangent vector and $\mathbf{n} \equiv \mathbf{k} \times \mathbf{s}$ is the unit normal vector (**k** directed upward). The streamline curvature $\kappa \equiv \mathbf{k} \cdot \nabla \times \mathbf{s}$ is defined positive for cyclonically curved flow; $R \equiv k^{-1}$ is the radius of streamline curvature. The horizontal gradient vector in the reference frame (**s**, **n**) takes the form $\nabla = \mathbf{s}\,\mathbf{s} \cdot \nabla + \mathbf{n}\,\mathbf{n} \cdot \nabla$. Directional (or intrinsic) derivatives are defined by $\delta/\delta s \equiv \mathbf{s} \cdot \nabla$ and $\delta/\delta n \equiv \mathbf{n} \cdot \nabla$, which are coordinate-independent operators. In the frame (**s**, **n**) the vertical component of the relative vorticity is expressed as $\zeta = -\delta v/\delta n + kv$, that is, shear and curvature vorticity, respectively (hereinafter denoted ζ^s and ζ^c). Figure 2 shows ζ^s and ζ^c separately, where it is observed that ζ^s is larger than ζ^c in the AJ. Water parcels traveling along the left edge (facing downstream) of the AJ have maximum positive ζ, while water parcels traveling along the right edge, between the AJ and the WAG, have zero or very small ζ. Therefore, along this right edge, positive ζ^s compensates for the negative ζ^c. A similar condition is also observed downstream of the crest in the EAG (Fig. 1b). It can be also observed from Figs. 1a,b that cross-jet ζ changes are larger than alongjet ζ changes; for example, the isoline of $\zeta = 0$ is almost coincident with the right limit of the AJ. The above dataset is, by now, the most adequate data for determining the ζ distribution of the AJ–gyres system. However, the positive vorticity nature of the AJ can also be observed from other datasets. For example, in July 1992 (Fig. 3) or during fall 1986 (see Fig. 13a in Tintoré et al. 1991), the isoline of $\zeta = 0$ ''encloses'' the WAG with the anticyclonically curving AJ having positive ζ.

The second point of this note, once we have determined that the AJ has positive ζ, deals with the alongjet changes in ζ, ζ^c, and ζ^s. Assuming steadiness it can be deduced that, when the AJ in the WAB acquires negative ζ^c ($\Delta\zeta^c \approx -0.5 \times 10^{-5}$ s^{-1} between 5° and 4.5°W at 100 m, Fig. 2b), it also acquires positive ζ^s ($\Delta\zeta^s \approx +1 \times 10^{-5}$ s^{-1} at 100 m, Fig. 2a), with the changes in ζ being therefore smaller ($\Delta\zeta \approx 0.5 \times 10^{-5}$ s^{-1} at 100 m, Fig. 1a). From the above results it seems that the vorticity changes in water elements traveling eastward between 5° and 4.5°W can be described as a ζ^c–ζ^s conversion. In the next section we identify, in a qualitative and a quantitative way, the main terms involved in such ζ^s–ζ^c conversion.

3. Shear vorticity–curvature vorticity conversion

The conversion between ζ^c and ζ^s (recall that now the terms velocity, vorticity, etc. include also the ageostrophic part) has been described using different formulations (Hollmann 1958; Chew 1974; Bleck 1991; see Viúdez and Haney 1996 for a review) and has been used to interpret both oceanographic and meteorological events (Chew 1974; Pitchler and Steinacker 1987; Bell and Keyser 1993). This conversion is described by means of the tendency equations for these quantities (the ζ^s–ζ^c equations). The interchange terms are the terms in these equations that modify the ζ^c and ζ^s of the fluid element in opposite senses; that is, they do not modify ζ. Chew (1974, 1975) applied the ζ^s–ζ^c equations to the Florida Current. Bell and Keyser (1993) extended the partition of the vorticity equation into shear and curvature components to the isentropic form of Ertel's potential vorticity equation and used both vorticity conversion and potential vorticity conversion equations to study a cutoff atmospheric cyclone event. Our study is based on ζ^s–ζ^c conversion rather than potential vorticity conversion because the relative vorticity, being a kinematical quantite independent of thermodynamic variables, is a simpler quantite to interpret. A detailed analysis of the potential vorticity in a reduced area of the AJ can be found in Viúdez et al. (1996a).

Since the ζ^s–ζ^c equations have been expressed in different ways, different expressions exist for the interchange term. We will use the form first derived by Hollmann (1958) and discussed by Viúdez and Haney (1996). For completeness we introduce first the components of the frictionless horizontal momentum equation in the (**s**,**n**) reference frame

$$dv/dt = -\delta\phi/\delta s, \tag{1}$$

$$v\mathbf{ds}/dt = -(fv + \delta\phi/\delta n)\mathbf{n}, \tag{2}$$

where $d/dt = \partial/\partial t + v\delta/\delta s + w\partial/\partial z$ is the material derivative and ϕ is the geopotential. The resulting ζ^c and ζ^s equations are

$$\frac{\mathrm{d}\zeta^c}{\mathrm{d}t} = -\frac{\delta^2\phi}{\delta n \delta s} + fv^{-1}v^a_{(s)}D^s - (f + \zeta^c)D - v\mathbf{n}\cdot\frac{\partial \mathbf{s}}{\partial z}\frac{\delta w}{\delta s} - \mathbf{v}\cdot\nabla f, \tag{3}$$

$$\frac{\mathrm{d}\zeta^s}{\mathrm{d}t} = \frac{\delta^2\phi}{\delta n \delta s} - fv^{-1}v^a_{(s)}D^s - \zeta^s D + \frac{\partial v}{\partial z}\frac{\delta w}{\delta n}. \tag{4}$$

In the above, $D = D^s + D^d$ is the horizontal divergence, and $D^s \equiv \mathbf{s} \cdot \nabla v$ and $D^d \equiv v\nabla \cdot \mathbf{s}$ are the speed- and direction-divergence, respectively. The quantity $v^a_{(s)}$ is the alongstream component of the ageostrophic velocity $\mathbf{v}^a \equiv \mathbf{v} - \mathbf{v}^g = v^a_{(s)}\mathbf{s} + v^a_{(n)}\mathbf{n}$. In the above equations the interchange terms (first two terms on the rhs) are kinematically independent of the ζ^s and ζ^c tendencies and do not include time derivatives. Furthermore, the ageostrophic nature of every term in the rhs of these equations is explicitly expressed. Note that $\delta\phi/\delta s = v^{-1}\mathbf{v} \cdot \nabla_h\phi$ is an ageostrophic quantity since the geostrophic velocity is perpendicular to the geopotential gradient. The first and second terms on the rhs of (3) and (4) have opposite signs in the two equations. They do not alter the ζ of the water parcel and therefore describe the transformation from ζ^s to ζ^c, and vice versa. The third term in (3) and (4) is the $(\zeta^c + f)$-divergence and the ζ^s-divergence term (or stretching term), respectively. The fourth is the tilting term, and the last term in (3) is the advection of planetary vorticity (or β term). The

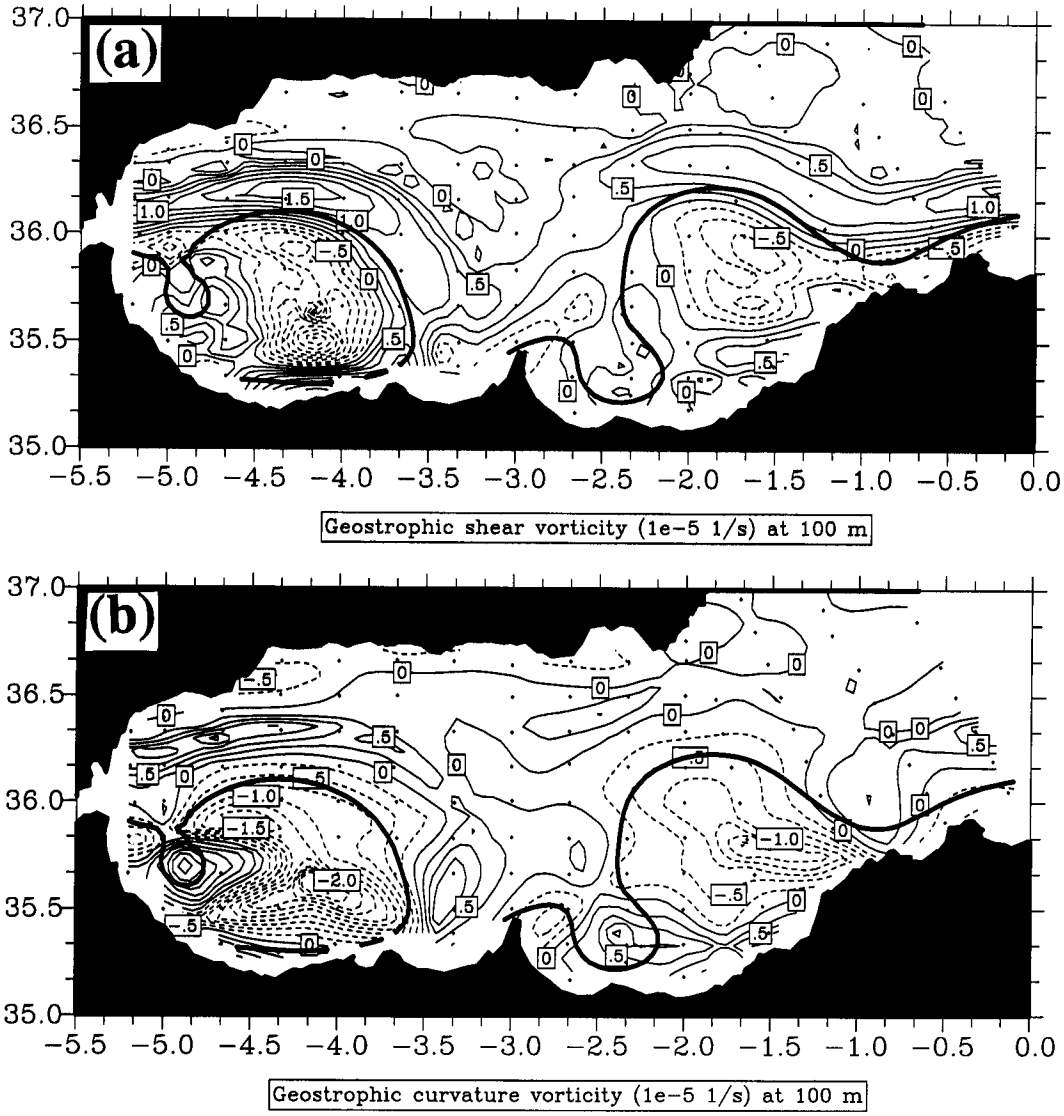

FIG. 2. (a) Geostrophic shear vorticity, $-\delta v^g/\delta n^g$, and (b) geostrophic curvature vorticity $\kappa^g v^g$ at 100 m. The contour interval is $\Delta = 0.25 \times 10^{-5}$ s^{-1}. Solid contour lines indicate positive (or zero) vorticity values. A geostrophic streamfunction isoline (thick curve) separating the Atlantic jet and Alboran gyres has been superimposed to specify their locations in the vorticity fields.

most important interchange term in our computations is $\delta^2\phi/\delta n\delta s$. The dynamical effect of this term is, from (1), to produce horizontal cross-stream gradients of the downstream acceleration.[1] In the AJ north of the WAG, the horizontal cross-stream gradients of dv/dt are enhanced (i) by the presence of MW flowing westward and, therefore, producing a counterflow (say at 100 m depth) on the left edge of the jet and (ii) by the increase of downstream acceleration on the right edge of the jet due to the streamline confluence (confluence of the AJ and WAG streamlines).

In order to compute every term on the rhs of (3)–(4) from the density data, we first obtained an adjusted, dynamically balanced three-dimensional velocity field by dynamical assimilation of the density data in a PE model (Viúdez et al. 1996b) using the technique of digital filter initialization (Lynch and Huang 1992). This method provides a dynamically balanced density and three-dimensional velocity field at the grid points of a $50 \times 40 \times 48$ regular matrix ($\delta x \approx 9.3$ km, $\delta y \approx 6.7$ km, $\delta z = 4$ m) covering the entire Alboran Sea. The most important term on the rhs of (3) and (4) is $\delta^2\phi/\delta n\delta s$ [$O(10^{-10}$ s$^{-2})$], followed by the $(\zeta^c + f)$-divergence

[1] The reader is referred to Chew (1974), Bell and Keyser (1993), and Viúdez and Haney (1996) for an extensive physical interpretation of the interchange terms.

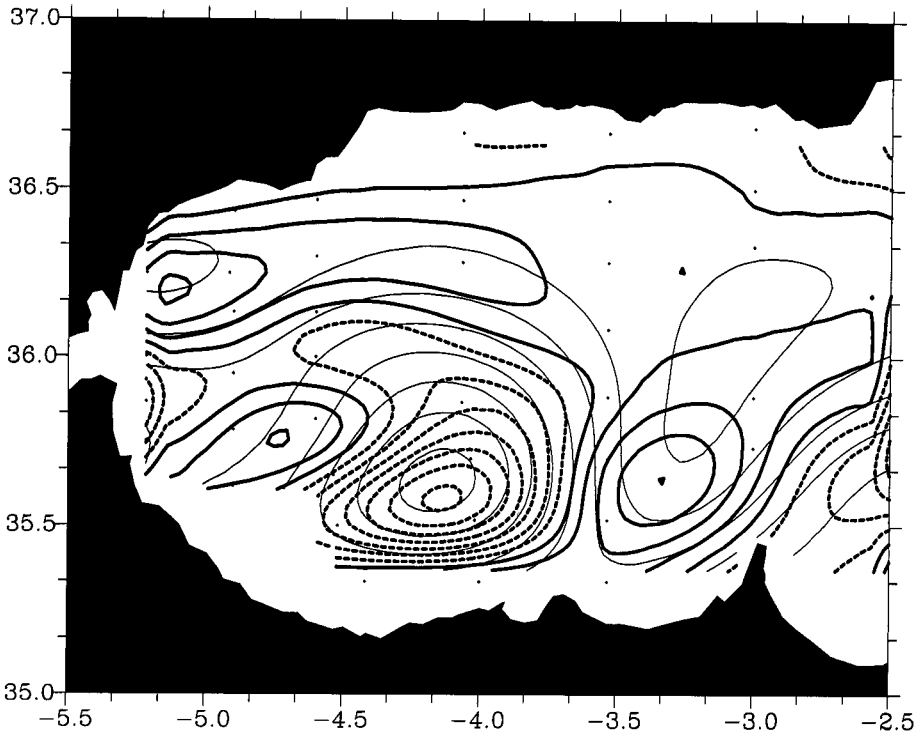

FIG. 3. Geostrophic streamfunction (thin lines) and geostrophic relative vorticity [thick isolines, solid for positive (or zero) values, with $\Delta = 1 \times 10^{-5}$ s^{-1}] at 10 m, from density data obtained in July 1992, that is, two months before the main dataset used in the text (Rubin et al. 1994). The dots indicate the CTD stations. Note that the AJ has mainly positive relative vorticity. The objective analysis used was a method of successive corrections (Brathset 1986; Franke 1988) using weight functions with a characteristic scale of 40 km.

term due to f (up to 0.5×10^{-10} s^{-2} in the AJ). At 100 m, the term $\delta w/\delta n \partial v/\partial z$ is $O(10^{-11}$ s$^{-2})$, while the ζ^s-divergence, $v\delta w/\delta s\mathbf{n}\cdot\partial\mathbf{s}/\partial z$, and the β terms are $O(10^{-12}$ s$^{-2})$. Although the term $fv^{-1}v^a_{(s)}D^s$ acquires maximum values up to 10^{-10} s^{-2} associated with the mesoscale eddies in the WAG, it is at least one order of magnitude smaller than $\delta^2\phi/\delta n\delta s$ in the AJ.

As a result of the above considerations, $\delta^2\phi/\delta n\delta s$ is considered the only significant interchange term. The importance of this term in relation to the other terms on the rhs of (3)–(4) may be quantified by comparison with the interchange *quantity*. The interchange quantity I_Q is defined as one-half the amount of vorticity tendency that is cancelled when the tendencies of ζ^c and ζ^s are added:

$$I_Q \equiv \text{sgn}\left(\frac{d\zeta^c}{dt}\right) \times \frac{1}{2}\left(\left|\frac{d\zeta^c}{dt}\right| + \left|\frac{d\zeta^s}{dt}\right| - \left|\frac{d\zeta}{dt}\right|\right) \quad (5)$$

(Viúdez and Haney 1996). By comparing $\delta^2\phi/\delta n\delta s$ with $-I_Q$ (Figs. 4a,b), it is concluded that the positive values of $-I_Q$ between 5° and 4.5°W at 36°N are due to the term $\delta^2\phi/\delta n\delta s$. In some other areas of the WAG that are not of interest in this study, $\delta^2\phi/\delta n\delta s$ differs from $-I_Q$. In Fig. 4a positive values represent a transfer of vorticity from ζ^c to ζ^s (i.e., a decrease in ζ^c and an increase in ζ^s). This term $\delta^2\phi/\delta n\delta s$ reaches a relative minima downstream of the pressure ridges, where the ζ^c of the fluid parcels is increasing most rapidly, and relative maxima immediately upstream of the ridges. For the purpose of this note we may focus on the positive interchange values in the AJ east of the Strait of Gibraltar between 5° and 4.5°W. Water parcels in the AJ crossing this area therefore experience a ζ^c decrease and a ζ^s increase. The distribution of ζ^c and ζ^s in this area of the AJ (Fig. 2), showing an increase of ζ^s and a decrease of ζ^c along the flow, is consistent with this interchange pattern.

In order to better quantify and visualize the vorticity and interchange terms in (3) and (4) we have computed such terms along streamlines. Four different sets of AJ streamlines were analyzed. Each particular streamline set is formed by streamlines beginning at the same horizontal location (x,y) but at different depths. The four streamline sets, denoted S1, S2, S3, and S4 (Fig. 5), are 200 km long. Each set originates at the exit of the Strait of Gibraltar, and follows the AJ in the WAB. Observe that, on the one hand, S1 ''begins'' in the AJ but, since it continues with negative ζ^c when close to the African coast, it ''ends'' in the WAG (this point will be addressed later). On the other hand, S4 have streamlines that ''U-turn'' to the left of the AJ due to the large ζ^s

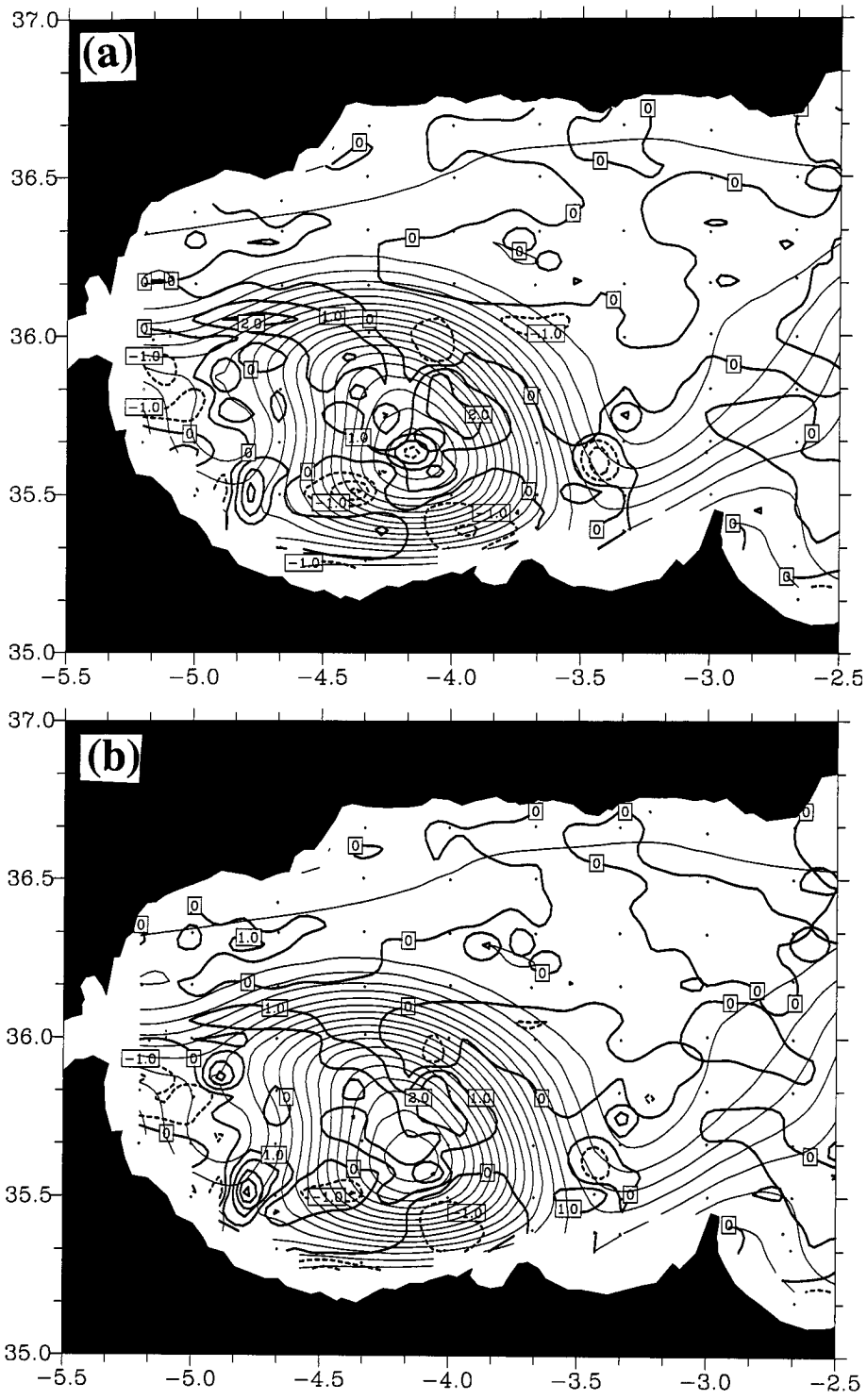

FIG. 4. Distribution of (a) the interchange term, $\delta^2\phi/\delta n\delta s$, and (b) the interchange quantity, $-I_Q$, at 100 m in the WAB. Note the relatively large positive values between 5° and 4.5°W at 36°N, where the AJ changes from positive to negative curvature at the exit of the Strait of Gibraltar ($\Delta = 1 \times 10^{-10}$ s^{-2}).

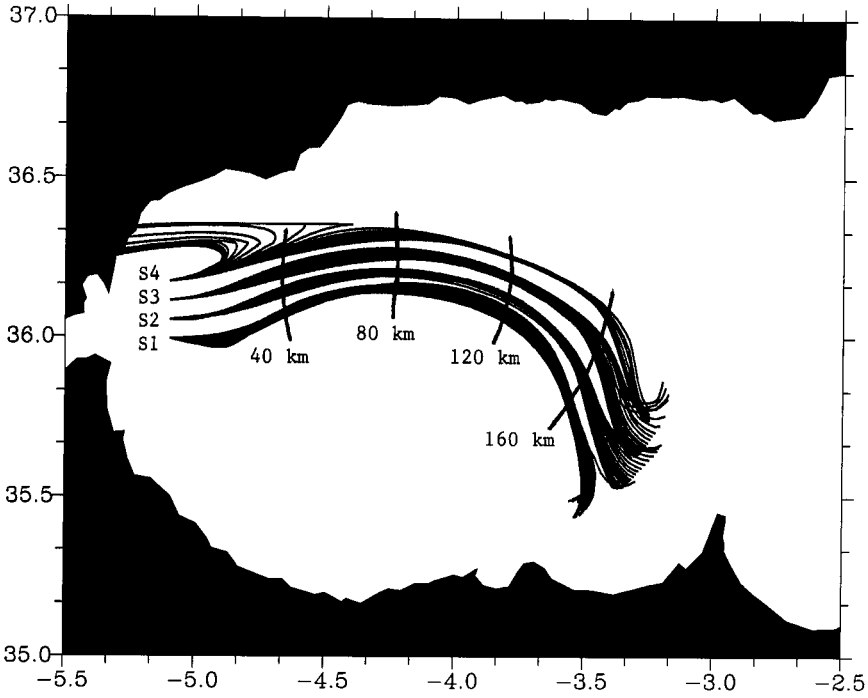

FIG. 5. Top view, or horizontal projection, of several streamline sets (S1, S2, S3, and S4) analyzed in the text. S1 and S4 correspond to the right and left limit (facing downstream), respectively, of the AJ. There are 27 streamlines in each set, beginning at different grid points separated by 4 m in the vertical from 18 m to 122 m. All streamlines (except those that intersect the coast) are 200 km long. Relative distance along streamlines is also indicated (in km).

in this area. These S4 streamlines are evidently unstable for the present data and numerical resolution (in the sense that initially vertically aligned streamlines experience large bifurcations), and will not be used. Therefore, S1 and S4 can be considered as representative of the right and left edge respectively, facing downstream, of the AJ. The S2 and S3 sets, located between S1 and S4, can then be considered representative of the AJ proper. We now use these streamline sets to analyze the alongjet and cross-jet variability of the vorticity and interchange terms along the AJ.

The ζ, ζ^s, ζ^c and interchange for S1, S2, and S3 are shown as a function of distance along the streamline in Fig. 6. A decrease in ζ^c is observed in almost every streamline between 10 and 60 km. All along the AJ between 30 and 180 km, with some exceptions in S3, the ζ^c is negative with typical values of $\approx -0.5 \times 10^{-5}$ s^{-1}. This evolution of the ζ^c along the streamlines is also evident from the curvature of the streamlines in Fig. 5. The ζ^s of particles on streamlines increases between 20 and 80 km, with some exceptions in S3 at depth 80 m, and remains positive for all the AJ streamlines bordering the WAG. Since the magnitude of ζ^s is larger than that of ζ^c, the ζ remains positive. Note the large cross-jet differences in ζ^s by comparing the ζ^s values for S1, S2, and S3 at the same depth and also taking into account that the initial horizontal distance between adjacent streamline sets is only 6.7 km, a small distance compared to the streamlines length (200 km).

The interchange term is generally positive for streamlines between 10 and 60 km, coincident with the decrease of ζ^c and the increase of ζ^s. The vorticity exchange occurs in such a way that the change of ζ along streamlines mimics the change in ζ^s except at a lower magnitude because of the simultaneous decrease of ζ^c. An order of magnitude estimate of the expected variation in ζ^c can be obtained from (3). For a downstream average value of the interchange term between 20 and 60 km at 100-m depth on the S2 streamline of 1×10^{-10} s^{-2} and a mean speed $v = 0.25$ m s^{-1} (Fig. 7), it follows from (3) that $\Delta(\kappa v)/\Delta s \approx -4 \times 10^{-10}$ m^{-1} s^{-1}. Thus, for $\Delta s = 0.4 \times 10^5$ m, we get $\Delta(\kappa v) \approx -1.5 \times 10^{-5}$ s^{-2}, which is consistent with the observed decrease of ζ^c and therefore supports the description in terms of the ζ^s-ζ^c conversion.

In the last part of the streamlines, between 160 and 200 km, the water parcels approach the African coast. The S2 and S3 streamline sets experience a decrease of ζ^s and an increase of ζ^c. Relative vorticity continues being positive, but now it is dominated by the positive ζ^c. In a simplified and global way, the large-scale behavior of S2 between 20 and 200 km has a $\cap$ shape for the ζ^s, but a $\cup$ shape for the ζ^c, the relative vorticity being always positive. On the other hand, S1 has aban-

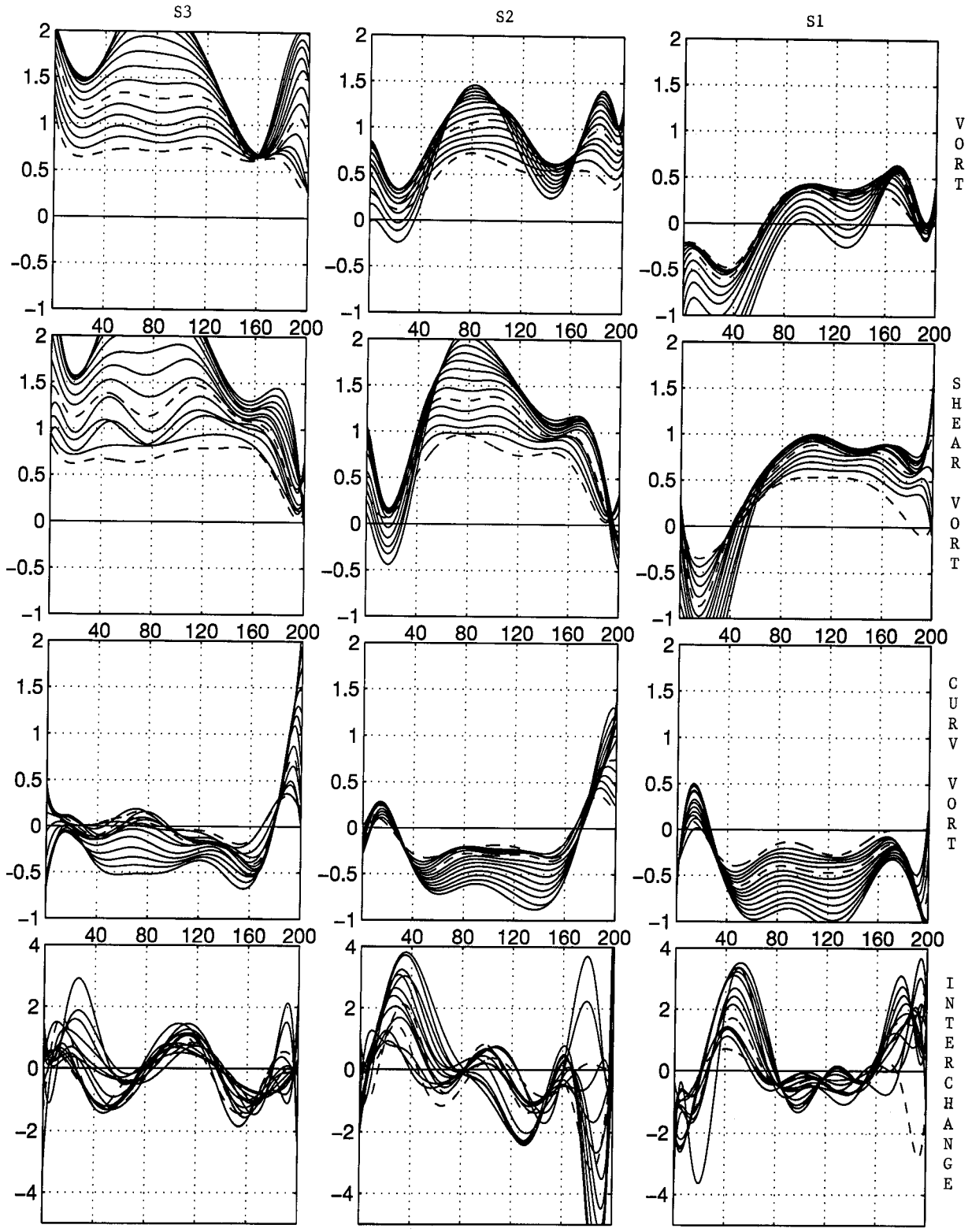

FIG. 6. From top to bottom, relative vorticity (ζ), shear vorticity (ζ^s), curvature vorticity (ζ^c) (in 10^{-5} s^{-1}), and interchange term (in 10^{-10} s^{-2}) for streamline sets S3, S2, and S1 (from left to right). There are 14 streamlines shown in each set, initially located at the same horizontal grid points but separated 4 m in the vertical from 70 to 122 m. All streamlines are 200 km long. The dashed lines correspond to the streamlines initially located at 100-m and 122-m depths.

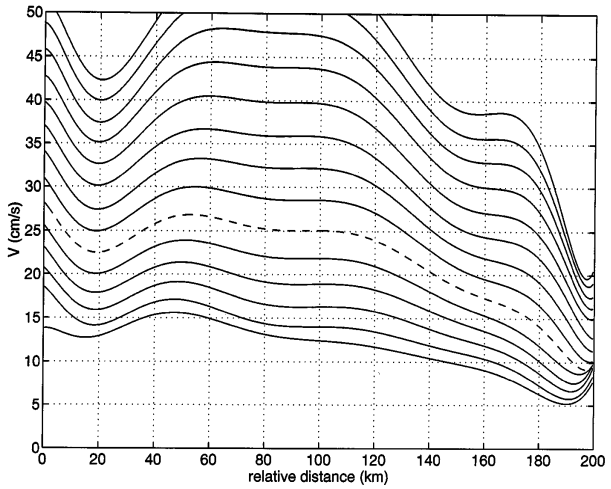

FIG. 7. Speed at streamlines S2, initially located between 70-m and 122-m depth. The dashed line corresponds to the streamline initially located at ~100-m depth.

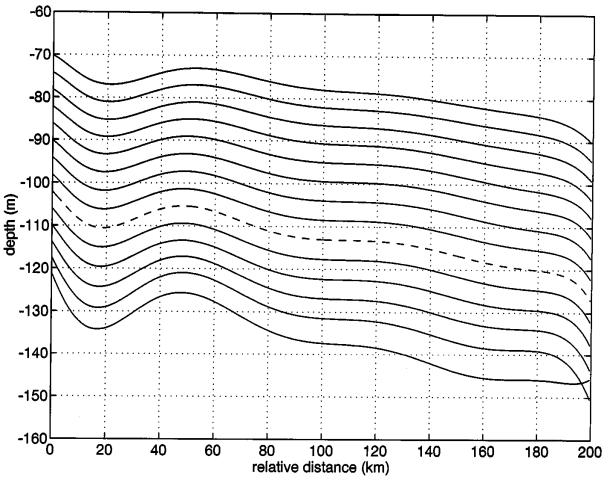

FIG. 8. Depth of streamlines S1, initially located between 70-m and 122-m depth. The discontinous line corresponds to the streamline initially located at ≈100-m depth. Note the large-scale downward displacement of $\Delta z \approx 20$ m over the full 200-km length of the streamline.

doned the AJ and has become part of the WAG. This behavior of S1 is partially due to the ageostrophic velocity, which is directed toward the center of the WAG along the right edge of the AJ (Viúdez et al. 1996a). In this region S1 streamlines are descending (Fig. 8) and, since they move over approximately isopycnal surfaces, the ageostrophic motion is downward and toward the right.

We now estimate the relative importance of the temporal variability in the observed quasi-synoptic values of the interchange term. The short-scale time variability of the AJ is dominated by transverse waves or oscillations of 9-day period (Perkins et al. 1990). These AJ oscillations are probably related (although not yet demonstrated) to fluctuations with approximately a 10-day period observed in the atmospheric pressure in the Western Mediterranean (Crépon 1965; Garrett 1983). Since typical cross-stream differences of ζ^c in the AJ are ~0.5 $\times 10^{-5}$ s^{-1} (Fig. 6), we estimate the local time variability of ζ^c as $\Delta\zeta^c/\Delta t \sim (0.5 \times 10^{-5}\ \text{s}^{-1})/(5\ \text{d}) \approx 10^{-11}\ \text{s}^{-2}$. This value is an order of magnitude smaller than the interchange values along streamlines between 10 and 60 km, where the vorticity conversion described in this note takes place.

4. Conclusions and discussion

From hydrographic data it has been shown that (i) the AJ in the Alboran Sea has zero or positive ζ, (ii) alongjet changes in ζ are smaller than the cross-jet changes, and (iii) the acquisition of negative ζ^c by the AJ at the exit of the Strait of Gibraltar coincides with an increase in both ζ^s and ζ. Consequently, a description based on ζ^s–ζ^c conversion has been used to characterize the curvature change of the wavelike front in the WAB. In this analysis, the acquisition of negative curvature by the AJ cannot be solely due to a direct (negative) forcing of ζ, which if anything, increases along the streamlines. We suspect, but cannot prove, that this increase of ζ^s along streamlines is mainly produced by turbulent momentum exchange between the eastward flowing AJ and the slower ''old'' MAW, or MW, that flows westward along the Iberian coast north of the AJ.

Chew (1974) referred to those meanders where the β effect is important compared to the advection of ζ^c in (3) as geostrophic meanders and those with negligible β effect as curvature-dominated meanders. The AJ, where the β effect is $O(10^{-12}\ \text{s}^{-2})$ and the advection of ζ^c is $O(10^{-10}\ \text{s}^{-2})$ [the order of magnitude of the rhs of (3)], is therefore a curvature-dominated meander, similar to the Loop Current, the West Florida Current, and the Florida Current analyzed by Chew (1974). In all the above meanders the $\delta^2\phi/\delta n\delta s$ and ζ^c-divergence terms were the most important ones in the ζ^c evolution equation (3). As commented by Chew (1974) *the dynamics of Rossby waves* (implying conservation of $f + \zeta^c$ by the fluid parcel) and *curvature-dominated meanders* are *opposite extremes* in the spectrum of meander dynamics implicit in (3). A difference between the AJ and the Florida Current is that ζ^s is positive at both crests and troughs in the AJ, while ζ^s and ζ^c have opposite signs at crests and troughs in the Florida Current. This difference may be due to the influence of the MW noted above. Such a MW influence is consistent with the results of Werner et al. (1988), who applied a reduced-gravity model to the Alboran Sea. Werner et al. found that the use of free-slip boundary conditions resulted in an unrealistic coastally trapped current on the Alboran southern boundary, while the use of no-slip boundary conditions caused the formation of a more realistic anticyclonic circulation upon the flow's entry into the WAB. In terms of vorticity, the no-slip condition tends

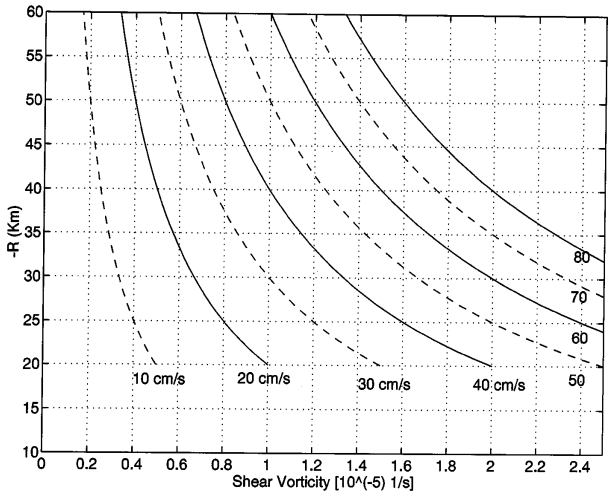

FIG. 9. Relationship between the radius of streamline curvature (R in km) and the shear vorticity ($-\delta v/\delta n$ in 10^{-5} s^{-1}), for different constant speed values, in the case when $-vR^{-1} = -\delta v/\delta n$.

to produce positive ζ^s along the northern part of the wavelike jet. Therefore, the role that such a boundary condition plays in the reduced-gravity model dynamics could be analogous to the role that MW plays in the Alboran Sea.

Some further conclusions about the size of the WAG can be drawn from the vorticity results obtained. If the isoline of zero relative vorticity is taken as representative of the boundary between the AJ and WAG, then conservation of $\zeta = 0$ along this isoline implies $\delta v/\delta n = R^{-1}v$. Therefore, if ζ^s at 100 m decreases [e.g., from 1 to 0.8 ($\times 10^{-5}$ s^{-1})] with constant $v = 30$ cm s^{-1}, then the radius of streamline curvature of the AJ–WAG edge should increase from 30 to 38 km (Fig. 9). If the horizontal velocity increases (e.g., from 30 to 40 cm s^{-1} at 100 m) with constant ζ^s (e.g., $-\delta v/\delta n \approx 1 \times 10^{-5}$ s^{-1}) then the curvature of the AJ–WAG limit should increase also from 30 to 40 km.

We must emphasize that, in our opinion, the vorticity conversion addressed here is just a *description* in terms of vorticity of the curvature change of the AJ, and should not be considered an *explanation* of it. Although the $\zeta^s - \zeta^c$ equations are often regarded as equations for the the $\zeta^s - \zeta^c$ interchange, the different terms in these equations in an inertial reference system ($f = 0$) are not Galilean invariant. Note that, because the directional derivatives $\delta/\delta s$ and $\delta/\delta n$ depend on **v**, the value of the *forcing* terms depend on the inertial observer. As a consequence, it makes no sense to state that, if ζ on a fluid element is conserved, changes in ζ^s *forces* changes in ζ^c, or vice versa. On the other hand, the vorticity conversion presented here describes a very specific property of the AJ, that is, its curvature change. Other characteristics of the AJ having shorter time and space scales — for example, short-term jet displacements (La Violette 1986), tide-induced fluctuations in the Strait of Gibraltar (La Violette and Lacombe 1988), or the observed splitting of the jet into several cores (Perkins et al. 1990)—are only accounted for in a time and space average sense.

Acknowledgments. We are grateful to J. Gil (IEO) for sharing the hydrographic data collected in July 1992 (Fig. 3) and to one reviewer for his constructive comments. A postdoctoral grant from the Ministerio Español de Educación y Ciencia, and support from the Office of Naval Research, are also gratefully acknowledged.

REFERENCES

Bell, G. D., and D. Keyser, 1993: Shear and curvature vorticity and potential vorticity interchanges: Interpretation and application to a cutoff cyclone event. *Mon. Wea. Rev.,* **121,** 76–102.

Bleck, R., 1991: Tendency equations for shear and curvature vorticity in coordinate-independent vector notation. *J. Atmos. Sci.,* **48,** 1124–1127.

Bormans, M., and C. Garrett, 1989: A simple criterion for gyre formation by the surface outflow from a strait, with application to the Alboran Sea. *J. Geophys. Res.,* **94**(C9), 12 637–12 644.

Brathset, A. M., 1986: Statistical interpolation by means of successive correction. *Tellus,* **38A,** 439–447.

Bryden, H. L., and H. M. Stommel, 1982: Origin of the Mediterranean outflow. *J. Mar. Res.,* **40,** 55–71.

Bucca, P. J., and T. H. Kinder, 1984: An example of meteorological effects on the Alboran Sea Gyre. *J. Geophys. Res.,* **89**(C1), 751–757.

Chew, F., 1974: The turning process in meandering current: A case study. *J. Phys. Oceanogr.,* **4,** 27–57.

——, 1975: The interaction between curvature and lateral shear vorticities in a mean and in an instantaneous Florida current, a comparison. *Tellus,* **27,** 606–618.

Crépon, M., 1965: Influence de la pression atmosphérique sur le niveau moyen de la Mediterranée occidentale et sur le flux à travers le détroit de Gibraltar. *Cah. Océanogr.,* **17,** 15–32.

Donguy, J. R., 1962: Hydrologie en mar d'Alboran. *Cah. Océanogr.,* **14,** 573–578.

Franke, R., 1988: Statistical interpolation by iteration. *Mon. Wea. Rev.,* **116,** 961–963.

Garrett, C. J. R., 1983: Variable sea level and strait flows in the Mediterranean: A theoretical study of the response to meteorological forcing. *Oceanol. Acta,* **6,** 79–87.

Gascard, J. C., and C. Richez, 1985: Water masses and circulation in the western Alboran Sea and in the Straits of Gibraltar. *Progress in Oceanography,* Vol. 15, Pergamon Press, 157–216.

Hollmann, G., 1958: Die Krümmungs- und die Scherungs-Vorticitygleichung; die Richtungs- und die Geschwindigkeits-Divergenzgleichung. *Beitr. Phys. Atmos.,* **30,** 254–267.

Klinger, B. A., 1994: Baroclinic eddy generation at a sharp corner in a rotating system. *J. Geophys. Res.,* **99,** 12 515–12 531.

Lanoix, F., 1974: Projet Alboran, Etude hydrologique et dynamique de la Mer d'Alboran. Tech. Rep. 66, NATO, Brussels, 39 pp. and 32 figures.

La Violette, P. E., 1986: Short-term measurements of surface currents associated with the Alboran Sea gyre during Donde Va? *J. Phys. Oceanogr.,* **16,** 262–279.

——, and H. Lacombe, 1988: Tidal-induced pulses in the flow through the Strait of Gibraltar. *Oceanol. Acta,* **9,** 13–27.

Loth, L., and M. Crépon, 1984: A quasi-geostrophic model of the circulation in the Mediterranean. *Remote Sensing of Shelf-Sea Hydrodynamics,* J.C.J. Nihoul, Ed., Elsevier Oceanogr. Ser., Vol. 38, Elsevier, 277–285.

Lynch, P., and X.-Y. Huang, 1992: Initialization of the HIRLAM model using a digital filter. *Mon. Wea. Rev.,* **120,** 1019–1034.

Marris, A. W., and S. L. Passman, 1968: Vector fields and flows on developable surfaces. *Arch. Ration. Mech. Anal.,* **31,** 29–86.

Ovchinnikov, I. M., V. G. Krivosheya, and L. V. Maskalenko, 1976: Anomalous features of the water circulation of the Alboran Sea during the summer of 1962. *Oceanology,* **15,** 31–35.

Parrilla, G., and T. H. Kinder, 1987: The physical oceanography of the Alboran Sea. NORDA Rep. 184, 26 pp.

Perkins, H., T. Kinder, and P. E. La Violette, 1990: The atlantic inflow in the western Alboran Sea. *J. Phys. Oceanogr.,* **20,** 242–263.

Pitchler, H., and R. Steinacker, 1987: On the synoptics and dynamics of orographically induced cyclones in the Mediterranean. *Meteor. Atmos. Phys.,* **36,** 108–117.

Preller, R. H., 1986: A numerical study of the Alboran Sea Gyre. *Progess in Oceanography,* Vol. 16, Pergamon Press, 113–146.

——, and H. E. Hurlburt, 1982: A reduced gravity numerical model of circulation in the Alboran Sea. *Hydrodynamics of Semi-enclosed Seas,* J. C. J. Nihoul, Ed., Elsevier, 75–89.

Rubin, J. P., and Coauthors, 1994: El ictioplancton y el medio marino en los sectores norte y sur del mar de Alborán, en Julio de 1992. Instituto Español de Oceanografía Tech. Rep. 146, 92 pp. [Available from Centro Oceanográfico de Málaga (IEO), P.O. Box 285, 29640 Málaga, Spain.]

Seco, E., 1959: La capa de velocidad cero en el mar de Alborán. *Rev. Ceincas.,* **XXV,** 765–779.

Speich, S., 1992: Étude du forçage de la circulation océanique par les détroits: cas de la mer d'Alboran. Ph.D. dissertation, Université Paris VI, 245 pp.

Tintoré, J., D. Gomis, S. Alonso, and G. Parrilla, 1991: Mesoscale dynamics and vertical motion in the Alboran Sea. *J. Phys. Oceanogr.,* **21,** 811–823.

Viúdez A., and R. L. Haney, 1996: On the shear and curvature vorticity equations. *J. Atmos. Sci.,* **53,** 3384–3394.

——, J. Tintoré, and R. L. Haney, 1996a: Circulation in the Alboran Sea as determined by quasi-synoptic hydrographic observations. Part I: Three-dimensional structure of the two anticyclonic gyres. *J. Phys. Oceanogr.,* **26,** 684–705.

——, R. L. Haney, and J. Tintoré, 1996b: Circulation in the Alboran Sea as determined by quasi-synoptic hydrographic observations. Part II: Mesoscale ageostrophic motion diagnosed through density dynamical assimilation. *J. Phys. Oceanogr.,* **26,** 706–724.

Wang, D.-P., 1987: The strait surface outflow. *J. Geophys. Res.,* **92**(C10), 10 807–10 825.

Werner, F. E., A. Cantos-Figuerola, and G. Parrilla, 1988: A sensitivity study of reduced-gravity channel flows with application to the Alborán Sea. *J. Phys. Oceanogr.,* **18,** 373–383.

Whitehead, J. A., and A. R. Miller, 1979: Laboratory simulation of the gyre in the Alboran Sea. *J. Geophys. Res.,* **84**(C7), 3733–3742.